Computer Physics Communications 180 (2009) 651–655

Contents lists available at ScienceDirect

Computer Physics Communications

www.elsevier.com/locate/cpc

Two-dimensional simulations of the amplification and focusing of intense laser pulses in the kinetic regime of Raman backward amplification in plasmas

Min Sup Hur [a,*], Jonathan S. Wurtele [b]

[a] UNIST, BanYeon-Ri 194, Ulsan, 689-805, Republic of Korea
[b] Department of Physics, University of California Berkeley and Center for Beam Physics, Lawrence Berkeley National Laboratory, Berkeley, CA 94720, USA

ARTICLE INFO

Article history:
Received 30 September 2008
Received in revised form 5 January 2009
Accepted 15 January 2009
Available online 22 January 2009

PACS:
42.65.Yj
52.38.Bv

Keywords:
Raman scattering
Plasma simulation
Amplification

ABSTRACT

Focusing of an intense laser pulse produced by backward Raman pulse amplification (BRA) has been numerically studied using a two-dimensional, axisymmetric kinetic model. The two-dimensional averaged particle-in-cell (aPIC) simulation assumes slowly varying field envelopes and is comprised of one-dimensional sub-models that are coupled radially through laser diffraction. A converging 33 TW seed pulse was amplified up to 1 PW. The focusing of the seed pulse, even when particle trapping was important, was maintained. It was also found that the focusing properties of the pulse tail can lead to some rewidening of the longitudinal pulse duration and some ideas for eliminating this effect were suggested. Simulations performed for various plasma densities and temperatures exhibited robust amplification and pulse shortening.

Currently, the shortest duration of ultraintense laser pulses from the chirped pulse amplification (CPA) technique is tens of fs for tens of terawatt pulses. A petawatt pulse can be generated from CPA, but, in that case, the pulse duration is generally hundreds of femtoseconds and the size of the system is increased so as to keep the gratings below their damage threshold. Laser pulse compression using backward Raman amplification (BRA) in a plasma was investigated [1–5] as means to realize ultra-high short pulses in a compact system.

One important feature of BRA is that the plasma is free from material damage thresholds. However, other plasma physics limitations become important (see [3] and references therein). Kinetic effects such as electron trapping and wavebreaking can lessen the amplification [6]. In this regime, where kinetic effects become important, the three wave interaction stops in the rear of the amplified pulse due to plasma wave breaking [7,8], which can restrict pulse shortening and lead, under certain conditions, to some pulse lengthening after compression. The details of kinetic effects should be better understood. Most of the preceding studies of kinetic effects have been based on one-dimensional systems; there have been only a few studies on multi-dimensional systems in the kinetic regime [9].

Previous work has examined focusability of the BRA scheme [10,11] using a three-dimension three-wave model. The focusing properties of the seed were found to be robust to variations of a wide range of system parameters. In this study, we consider the focusability of the BRA in the regime where kinetic effects, in particular particle trapping and the associated nonlinear pulse detuning, are important.

Previously, we investigated the pulse shortening and amplification from interaction between a pump which is an intense, short (10^{16} W/cm^2, 900 fs) pulse and an even shorter and stronger counter-propagating seed pulse in a thin (~0.15 mm) plasma slab [7]. We studied the feasibility of BRA as a means to generate tens of terawatt and less-than-15 fs laser pulse, which is not readily available from the current CPA technique. The advantage of using a short pump and a thin plasma is that undesirable laser-plasma instabilities arising from long interaction such as pre-depletion of the pump by spontaneous Raman scattering and energy loss of the seed pulse by inverse Bremsstrahlung or Raman forward scatter [3], can be minimized. We observed pulse shortening from 31 fs into 15 fs [7] in a one-dimensional averaged particle-in-cell (aPIC) simulation [12]. Assuming a reasonable value for the unfocused spot size of the amplified seed pulse, we found the resultant power could reach tens of terawatt. Of course, the focusing of the amplified seed pulse could not be shown explicitly in a one-dimensional study.

In this paper, we investigate numerically the diffraction and focusing of the compressed pulse in a similar parameter regime by

* Corresponding author.
E-mail addresses: mshur@unist.ac.kr (M.S. Hur), JSWurtele@lbl.gov (J.S. Wurtele).

0010-4655/$ – see front matter
doi:10.1016/j.cpc.2009.01.013

extending the one-dimensional aPIC model to a cylindrically symmetric two-dimensional model. We believe this is the first use of the envelope-kinetic equations in two-dimensional BRA studies. The two-dimensional kinetic simulation demonstrate that, for short pump examples, kinetic effects are not deleterious to the focusing of the seed pulse. The BRA compression and focusing is robust to density and temperature variations.

However, we observed an undesirable feature of the focusing: some rewidening of the pulse duration at the propagation axis due to the focusing of the pulse tail.

Before we address the details of the simulations, we summarize the two-dimensional aPIC (envelope fields and kinetic particles) numerical model. The two-dimensional aPIC model is similar to the one-dimensional aPIC model. Explicitly, the laser pulse envelopes are

$$\frac{\partial a_1}{\partial t} + c\frac{\partial a_1}{\partial z} + i\frac{2c}{k_1}\nabla_\perp^2 a_1 = -i\frac{\omega_p^2}{2\omega_1}a_0\left\langle\frac{e^{i\phi_j}}{\gamma_j}\right\rangle, \tag{1a}$$

$$\frac{\partial a_0}{\partial t} - c\frac{\partial a_0}{\partial z} - i\frac{2c}{k_0}\nabla_\perp^2 a_0 = -i\frac{\omega_p^2}{2\omega_0}a_1\left\langle\frac{e^{-i\phi_j}}{\gamma_j}\right\rangle, \tag{1b}$$

where k_0 and k_1 are the wavenumbers of the seed and pump pulses, respectively, the subscript j is the simulation particle index, ϕ_j is the jth particle's ponderomotive phase defined by $-(k_0+k_1)z_j-(\omega_0-\omega_1)t$, and the bracket refers to an ensemble average over particles. Subscripts 0 and 1 represent the pump and seed, respectively. Note that, in this model, the difference between the one-dimensional equations [12] is that the diffraction terms are added in the envelope equations. The equation of motion for plasma electrons is

$$\frac{\mathrm{d}\gamma_j\vec{v}_j}{\mathrm{d}ct} = -\frac{e\vec{E}_j}{mc} - c\nabla\gamma_j, \tag{2}$$

where E_j is the electric field evaluated on the jth particle. The relativistic factor γ_j of the jth particle is defined by

$$\gamma_j = \sqrt{1+\frac{u_{z,j}^2}{c^2}+\frac{1}{2}|a_0|^2+\frac{1}{2}|a_1|^2+\Re e\left[\vec{a}_0\cdot\vec{a}_1^{*}e^{i\phi_j}\right]}, \tag{3}$$

where $a_{0,1}$ are the pulse envelopes measured at the position of the jth particle (z_j). Note that Eqs. (1)–(3) does not allow either the self-focusing of the laser pulses or pulse guiding by plasma channel, since the source terms in Eq. (1) do not include the self-current: the current comes from just the coupling of the two laser pulses. Enabling such effects remain to be improved. In this paper we consider the Raman interaction of unfocused pulses in uniform plasmas, where the laser intensity is quite below the relativistic regime. Thus the self-focusing or channel guiding do not matter here.

The moving window, where the simulation domain co-moves with the seed pulse with a speed of light, is employed to avoid the unphysical effects induced by the numerically enhanced thermal noise of the plasma; a fresh quiet plasma keeps being loaded at the moving window edge. The moving window also helps reduce the computation time, since the simulation domain can be small enough to cover up just the area occupied by the short seed pulse.

We solve Eqs. (1)–(3) subject to further simplifying assumptions: (i) the transverse electron current induced by the laser fields is assumed to be negligible compared to the longitudinal current; (ii) the important term in the electron motion is from the beat-wave ponderomotive force (the other ponderomotive forces are much weaker since they are driven by the scale of the full pulse envelope rather than the wavelength of the radiation) and (iii) the electrostatic wave can be modelled one-dimensionally.

The electrostatic plasma wave $\vec{E}_j$ in Eq. (2) is calculated from

$$\frac{\partial E}{\partial z} = -\frac{e(n-n_0)}{\epsilon_0}. \tag{4}$$

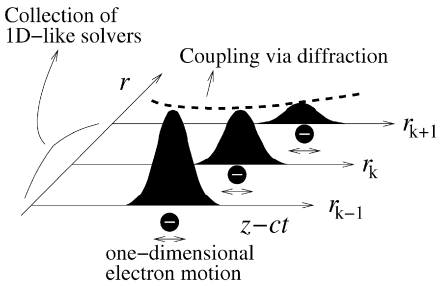

Fig. 1. Simulation model for axisymmetric RBS. At each radial position, r_k, the envelopes of the seed and pump pulses are modeled by slightly modified one-dimensional equations. The diffraction term couples the one-dimensional solvers.

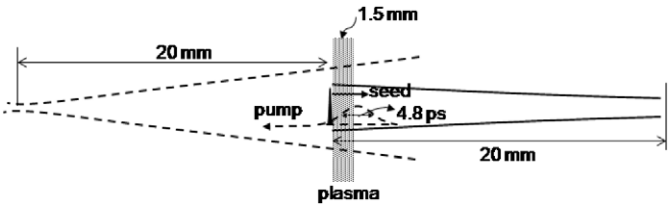

Fig. 2. The initial position of the pulses relative to the plasma and focusing.

The plasma density n in Eq. (4) is obtained from the simulation particles following conventional particle-in-cell methods [13]. Here n_0 is the immobile ion background density.

From these simplifying assumptions, the dynamics of electrons is considered to be confined in the z-direction only, with transverse oscillations determined by the local value of the vector potentials of the waves, so that

$$\frac{\mathrm{d}\gamma_j v_j}{\mathrm{d}ct} = -\frac{eE_j}{mc} - c\frac{\partial\gamma_j}{\partial z}. \tag{5}$$

A benefit of this formulation is that the evolution of the laser envelopes and plasma wave at each radial position can be studied using a solver very similar to that in the one-dimensional aPIC code. A one-dimensional envelope solver is used each radial position. At a specific radial position, the one-dimensional solver is coupled with adjacent solvers via the diffraction term. The numerical scheme is graphically presented in Fig. 1. Note that the equation of motion is only for the electrons, since the ion motion is negligible on the time scale of BRA.

Motivated by previous one-dimensional results [7], where 15 fs pulse compression was obtained, simulation parameters similar to those in Ref. [7] were chosen for these two-dimensional simulations. The plasma slab is 1.5 mm in axial length and uniform transversely. The plasma density and temperature are 2.8×10^{19} cm^{-3} and 10 eV, respectively. The wavelengths of the seed and pump pulses are 1.05 and 0.9 μm, respectively. The focal length of the seed pulse is 2 cm from the plasma slab and the waist at the focal point is 20 μm (FWHM). The peak amplitude a_1 at the focal point is set to be 2.45, so that its value inside the plasma (i.e., 20 cm before focusing) becomes approximately 0.11, which is similar to the seed amplitude used in Ref. [7]. Initial pulse duration of the seed pulse is 31 fs (FWHM). The pump pulse spot size (FWHM) is 10 μm at the focal point, which is 20 cm away from the plasma slab. The pump amplitude at focal point is $a_0 = 2.47$, which corresponds to $a_0 = 0.03$ inside the plasma slab. The pump pulse duration is 4.8 ps (FWHM). Note that the spot size of the pump pulse inside the plasma slab is 790 μm, which is wide enough to fully cover the seed pulse spot (470 μm). The relative initial location and focusing of the pulses are presented in Fig. 2. The domain size for the simulation is 1.2 mm × 0.05 mm in radial and longitudinal directions, respectively. The radial mesh size Δr is 1.94 μm and the longitudinal mesh is the same as the beat wavelength:

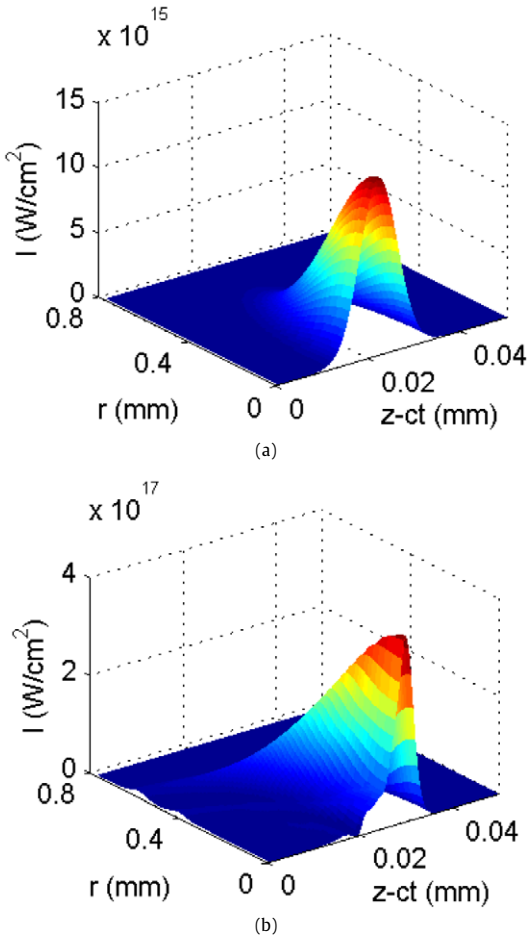

Fig. 3. Profiles of the seed pulse (a) before and (b) after the plasma slab. Note the modification to the radial profile, especially at the rear of the amplified pulse.

$\Delta z = \lambda_b = 0.485$ μm. For the calculation of the short wavelength plasma wave by Poisson equation, the longitudinal mesh is resolved [12] by the sub-mesh δz, where we set $\Delta z = 32\delta z$.

The seed pulse profile before entering the plasma slab and just after passing through the plasma is plotted in Fig. 3 (a) and (b), respectively. The pulse duration on the axis was shortened by BRA to 14 fs, and the peak intensity was 3.8×10^{17} W/cm^2, corresponding to the amplification factor of the peak intensity 27.7. The total pump energy was initially 59.3 J. The pump energy after BRA was measured to be 23.7 J, corresponding to the energy depletion by 60 percent.

In one-dimensional BRAs, the speed of the pulse propagation depends on the pulse shape and amplitude (see, for example, [14] for a discussion of how this can influence the BRA performance). Here, with a focusing pulse and transverse field variation, we expect this effect to lead to a transverse pulse shape to vary with axial position. This is seen in the bow-like shape (which looks like a bowl in a three-dimensional space) shown in Fig. 3(b). A similar pulse shape was observed in three-wave simulations [15] and a fully kinetic (PIC) simulation [9].

For comparisons we simulated the same parameters with the three wave model, where the source terms of Eqs. (1) are replaced by $-\frac{\omega_p}{2} f^* a_0$ and $\frac{\omega_p}{2} f a_1$, respectively [11]. Here f is the plasma wave envelope. Fig. 4 is the seed pulse shape just after passing through the plasma. The main pulse of the seed is followed by a train of sub-peaks, which is similar to the typical pi-pulse solution of the one-dimensional three-wave model [2]. The peak intensity and pulse duration at the axis are 4.15×10^{17} W/cm^2 and 10.9 fs, respectively. More pulse compression was obtained from the three-

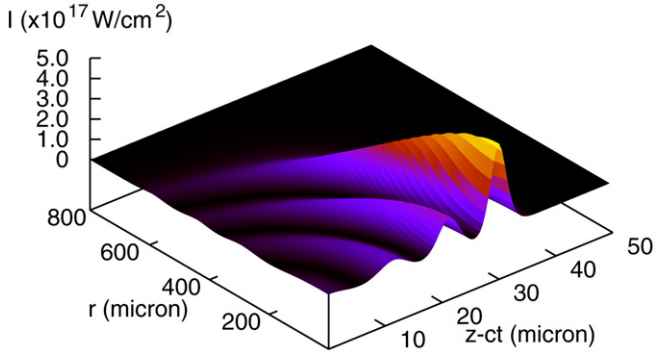

Fig. 4. The seed pulse just after RBS obtained from the three-wave model.

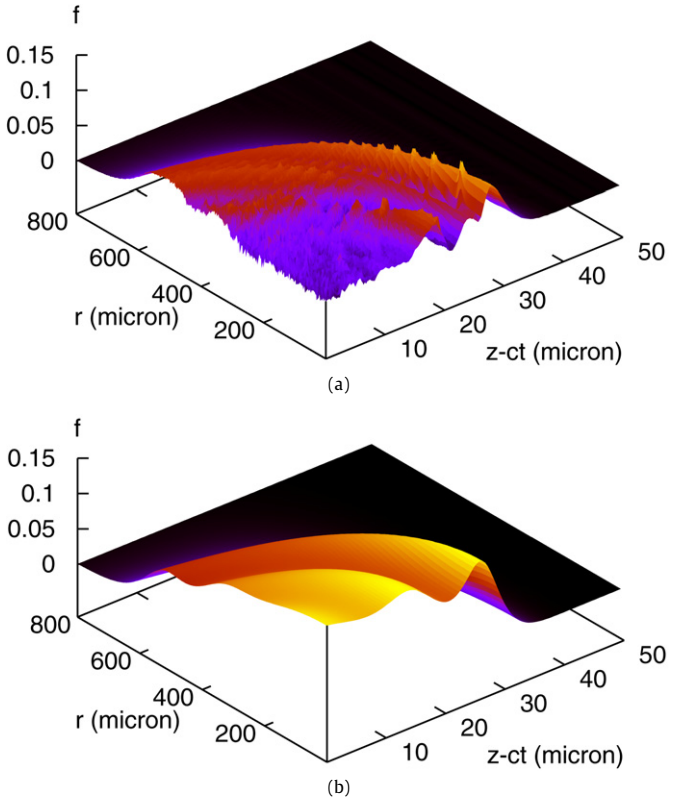

Fig. 5. The plasma wave envelopes from (a) the kinetic model and (b) the three-wave model.

wave model than from the kinetic model. The less compression in the kinetic model is due to the breaking of the plasma wave in the rear part of the seed pulse, where there exists no coherent plasma wave mediating the energy transfer between the seed and pump. This is shown clearly from the comparison of the plasma wave envelopes from two different models (Fig. 5). The plasma wave envelope f from the kinetic model looks prominent just near the front part of the seed, while that from the three-wave model keeps well its amplitude behind the seed pulse. The definition of the plasma wave envelope can be found in Ref. [6]. Fig. 6 shows that the electron flow is not laminar and trapping is significant. The trapping is observed not only on axis [Fig. 6(a)], but also in the off-axis region [Fig. 6(b)]. Note that the amplification operated in marginally superradiant regime [4]: the bounce frequency $\omega_B = 2\omega_1\sqrt{a_0 a_1}$, where ω_1 is the laser frequency, is nearly the same as the plasma frequency ω_p. In our case, $\omega_B \sim 3.08 \times 10^{14}$ and $\omega_p \sim 3 \times 10^{14}$. Note that u_z/c is the longitudinal velocity of electrons and the plasma wave is travelling to the left in the figure.

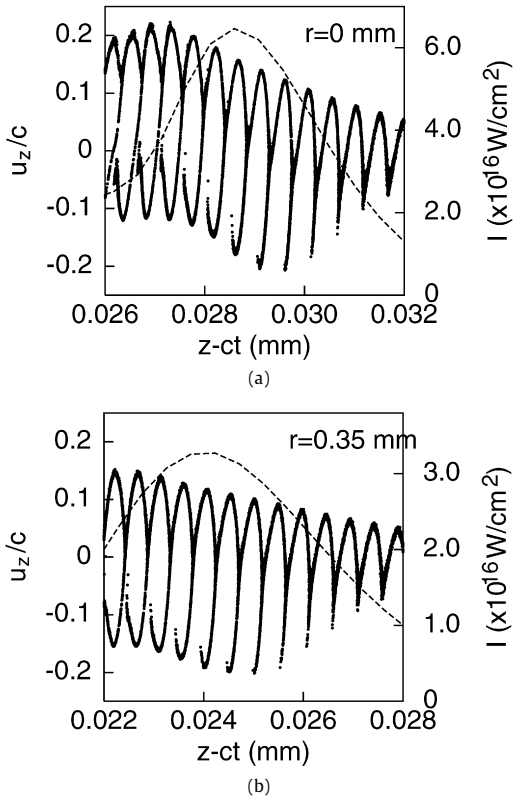

Fig. 6. Electron phase spaces inside the plasma, after the seed pulse propagated by 0.12 mm. The dashed lines represent the seed pulse profiles.

After passing through the plasma slab, the amplified seed pulse propagates in vacuum. In vacuum, a radial cut of the seed envelope at a given longitudinal position $z = z_0$, i.e. $a_1(z = z_0, r)$ (the 'slice') does not interact with other slices following it $[a_1(z < z_0, r)]$. In vacuum, since the slices move independently, the envelope equation (1) for the seed pulse can be reduced to

$$\frac{da_1}{dz} + \frac{i}{2k_1}\nabla_\perp^2 a_1 = 0. \tag{6}$$

To study the focusing of the amplified seed pulse, we selected 50 slices $[a_1(z = z_m, r),\ m = 1, \ldots, 50]$ from the seed pulse envelope presented in Fig. 3(b). The propagation of each slice by 2 cm (focal length) was calculated using Eq. (6) and the three-dimensional illustration of the seed pulse was reconstructed from the propagated slices (see Fig. 7). The spot size of the seed pulse just after RBS [Fig. 3(b)] is 600 μm in FWHM. During the propagation in vacuum, it shrank into 24.7 μm (Fig. 7). The peak intensity of the focused pulse is 1.26×10^{20} W/cm^2, which, combined with the final spot size at the focus, yields 0.87 PW. For this example, the power gain of the seed pulse is 30 compared to no BRA interaction.

Though the focusing of the seed pulse is well conserved, even after the RBS in the strong kinetic regime, there is an undesirable feature in longitudinal pulse duration: the rewidening of the pulse duration on the axis. The seed pulse duration at the propagation axis was 14 fs just after RBS [Fig. 3(b)]. After the propagation in vacuum by 1.9 cm, it widened to 32 fs. The rewidening of the pulse duration comes from the focusing of the pulse tail. The radial cut (slice) at the tail of the bowl-like pulse takes a hollow shape. The pulse energy concentrated at the rim of the hollow focuses into the near-axis region, resulting in the blow-up of the rear part of the seed pulse on the axis. Such an effect is well illustrated in Fig. 8, which represents the evolution of the slices at three different places. The hollow slice at $z - ct = 0.024$ mm changes into a bell-like shape [Fig. 8(b)] as the pulse focuses. Similar rewidening

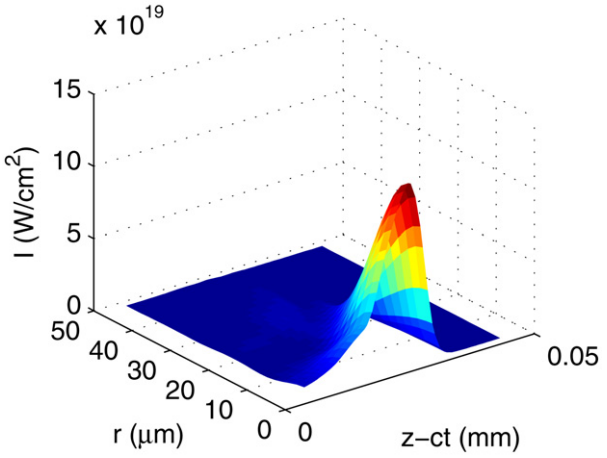

Fig. 7. Profile of the seed pulse near the focal point, 19 mm away from the plasma slab.

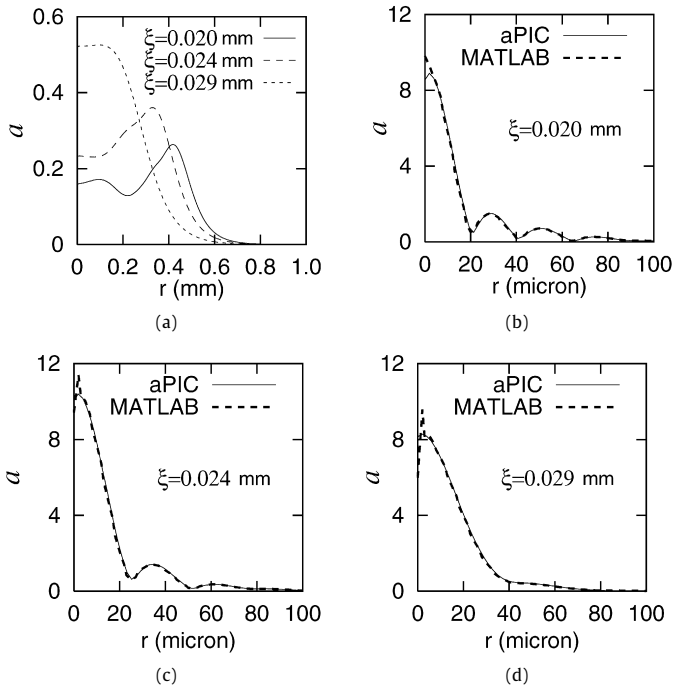

Fig. 8. Radial profiles of the seed pulse at various positions ($\xi = z - ct$); (a) immediately after passing through the plasma and (b), (c), (d) near the focal point. In (b), (c), (d), the MATLAB calculations are overlapped for comparison.

of the pulse by focusing was observed in the three-wave result. To benchmark the vacuum propagation solutions, we calculated the propagation using MATLAB. The results from two different envelope solvers are in excellent agreement with each other.

This study suggests that manipulation of radial variation of RBS process could enhance the performance of the BRA as an effective pulse compressor. For example, one might try a pump pulse with a peak power density off axis to flatten the Raman growth profile, so that the bowl-like shape lessens. Another idea is to use a plasma channel whose density off-axis is more resonant with the two counter-propagating pulses; we speculate that this, properly set up, could lead to improved pulse shape at the focus.

We studied the sensitivity of the pulse compression and focusing in the BRA to variations in density, temperature and seed wavelength. This is shown in Fig. 9, where the variation of the pulse length and energy are plotted for a range of parameters. In Fig. 9(a), the plasma density is varied by ±15% from resonance

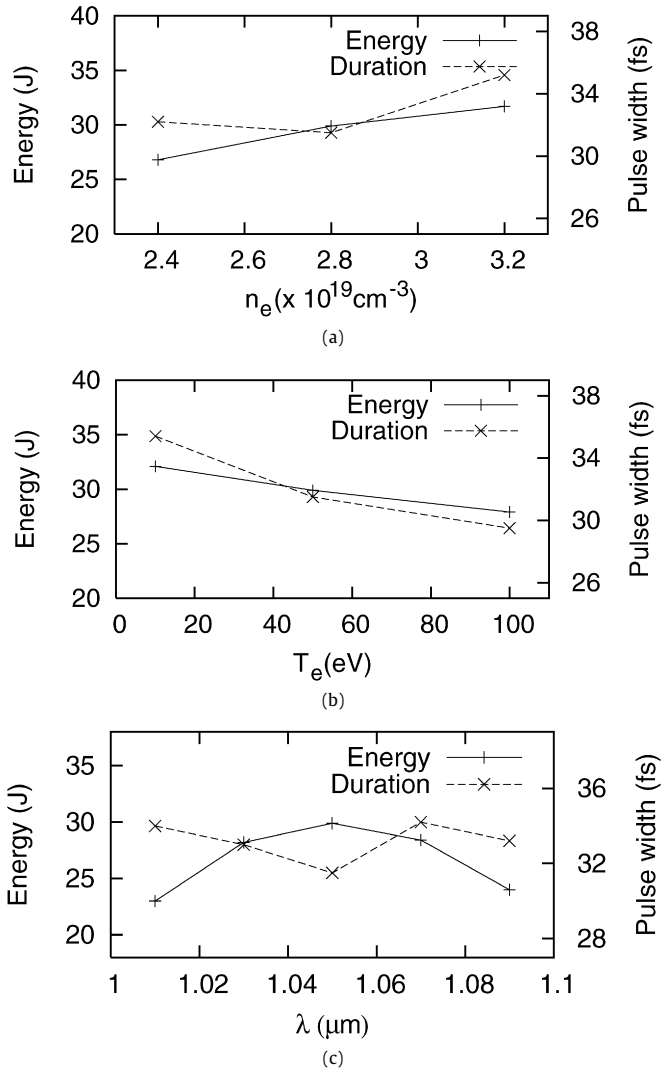

Fig. 9. The energy and pulse duration of the seed pulse for various plasma densities, temperatures, and seed wavelengths. Amplification is seen to be robust.

($\omega_p - \omega_0 + \omega_1 \simeq 0$ for $n_0 = 2.8 \times 10^{19}$ cm^{-3}), while the energy of the seed pulse after BRA exhibits less than a ±10% variation. This level of precision of density control should be obtainable with current technology. In Fig. 9(b) the plasma temperature is varied from 10–100 eV and in Fig. 9(c) the seed wavelength is varied; here the energy is reduce by about 8 change in wavelength of 2. Thus, the BRA performance is seen to be robust. Such robustness originates from the wide bandwidth of the extremely short seed pulse, which can compensate for detuning from resonance induced by the trapped particles, and density and temperature changes. Note that in the Raman regime, where the seed pulse length should be much longer, the Raman amplification is more sensitive to the variation of the plasma density and temperature (for instance, see Ref. [12]). The results in this paper are concerned with modeling short pulses. Further studies in the Raman regime, using the two-dimensional aPIC code described here, could be compared to three-wave predictions [10,11]. Benchmarking of the two-dimensional aPIC code with a full PIC simulation should be performed in order to identify the limits of the averaged model with transverse physics.

In summary, two-dimensional BRA has been modelled with cylindrically symmetric aPIC equations. In the first application of this a model, we investigated, in the kinetic regime, the focusing of an amplified seed pulse after BRA. As in the cold plasma limit, the BRA does not disrupt the seed pulse focusing after the plasma. Two-dimensional variations in RBS interactions can lead a hollow-shaped tail of the pulse which has different focal properties beyond the plasma, leading to a rewidening of the pulse duration as seen on axis. Several novel techniques to surmount such an effect were suggested. For other applications, such as modifying the radial property of ultra-intense laser pulses, such two-dimensional variations in the BRA coupling might be found to be useful. Simulations with a range of plasma densities and temperatures exhibited the desired robust behavior of the BRA system.

Acknowledgements

This work was supported by the 2008 Research Fund of UNIST (Ulsan National Institute of Science and Technology). This work was also supported by High Energy Division U.S. DOE under Contract no. DE-AC02-05CH11231 and the NNSA under the SSAA Program through DOE Research Grant No. DEFG5207NA28122.

References

[1] V.M. Malkin, G. Shvets, N.J. Fisch, Phys. Rev. Lett. 82 (1999) 4448.
[2] V.M. Malkin, G. Shvets, N.J. Fisch, Phys. Plasmas 7 (2000) 2232.
[3] D.S. Clark, N.J. Fisch, Phys. Plasmas 10 (2003) 3363.
[4] G. Shvets, N.J. Fisch, A. Pukhov, J. Meyer-ter-Vehn, Phys. Rev. Lett. 81 (1998) 4879.
[5] N.J. Fisch, V.M. Malkin, Phys. Plasmas 10 (2003) 2056.
[6] M.S. Hur, R.R. Lindberg, A.E. Charman, J.S. Wurtele, H. Suk, Phys. Rev. Lett. 95 (2005) 115003.
[7] M.S. Hur, J. Kim, D.N. Gupta, H.J. Jang, H. Suk, Appl. Phys. Lett. 91 (2007) 101501.
[8] M.S. Hur, D.N. Gupta, H. Suk, J. Phys. D 40 (2007) 5155.
[9] P. Mardahl, H.J. Lee, G. Penn, J.S. Wurtele, N.J. Fisch, Phys. Lett. A 296 (2002) 109.
[10] A.A. Solodov, V.M. Malkin, N.J. Fisch, Phys. Plasmas 10 (2003) 2544.
[11] A.A. Balakin, G.M. Fraiman, N.J. Fisch, V.M. Malkin, Phys. Plasmas 10 (2003) 4856.
[12] M.S. Hur, G. Penn, J.S. Wurtele, R.R. Lindberg, Phys. Plasmas 11 (2004) 5204.
[13] J.M. Dawson, Rev. Mod. Phys. 55 (1983) 403;
C.K. Birdsall, A.B. Langdon, Plasma Physics via Computer Simulation, Adam Hilger, Bristol, Philadelphia, and New York, 1991.
[14] Yu.A. Tsidulko, V.M. Malkin, N.J. Fisch, Phys. Rev. Lett. 88 (2002) 235004.
[15] G.M. Fraiman, N.A. Yampolsky, V.M. Malkin, N.J. Fisch, Phys. Plasmas 9 (2002) 3617.